

# Shielding for the ATLAS Experimental Region

11 September 1995  
srollet@dxcern

A. Ferrari\*, K. Potter<sup>+</sup> and S. Rollet<sup>+</sup>

\* INFN, Sez. di Milano, Via Celoria 16, 20133 Milan, Italy

<sup>+</sup> CERN, CH-1211 Geneva 23, Switzerland

Keywords: RADIATION PROTECTION, SHIELDING, ATLAS, POINT 1.

---

---

## 1. Introduction and summary

The shielding requirements for the ATLAS experimental region are computed using a realistic geometry description both for the detector and for the experimental cavern. The thickness of concrete required to reduce equivalent radiation doses to levels safely below accepted limits are computed for the lateral wall which separates the experimental and equipment caverns. The dimensions of the ducts carrying cables and pipes and all passages between the experimental cavern and the control rooms are also discussed. A detailed analysis of particle fluences up the two large access shafts is used to determine the correct thickness for the shielding plugs at the top. Estimates are then made of particle fluences and dose equivalents in the surface buildings and at the site limits.

In the present report the same ATLAS detector description presented by the collaboration in their Technical Proposal [1] has been adopted and inserted in a real experimental hall with a lateral flat wall and two vertical access shafts. This has then been used to compute:

- the thickness of the lateral vertical wall between the experimental cavern and the equipment and counting room cavern;
- the thickness of the concrete plugs at the top of the two vertical shafts;
- the fluence and dose rate in the surface buildings;
- the maximum dimensions allowed for the lateral passage ducts.

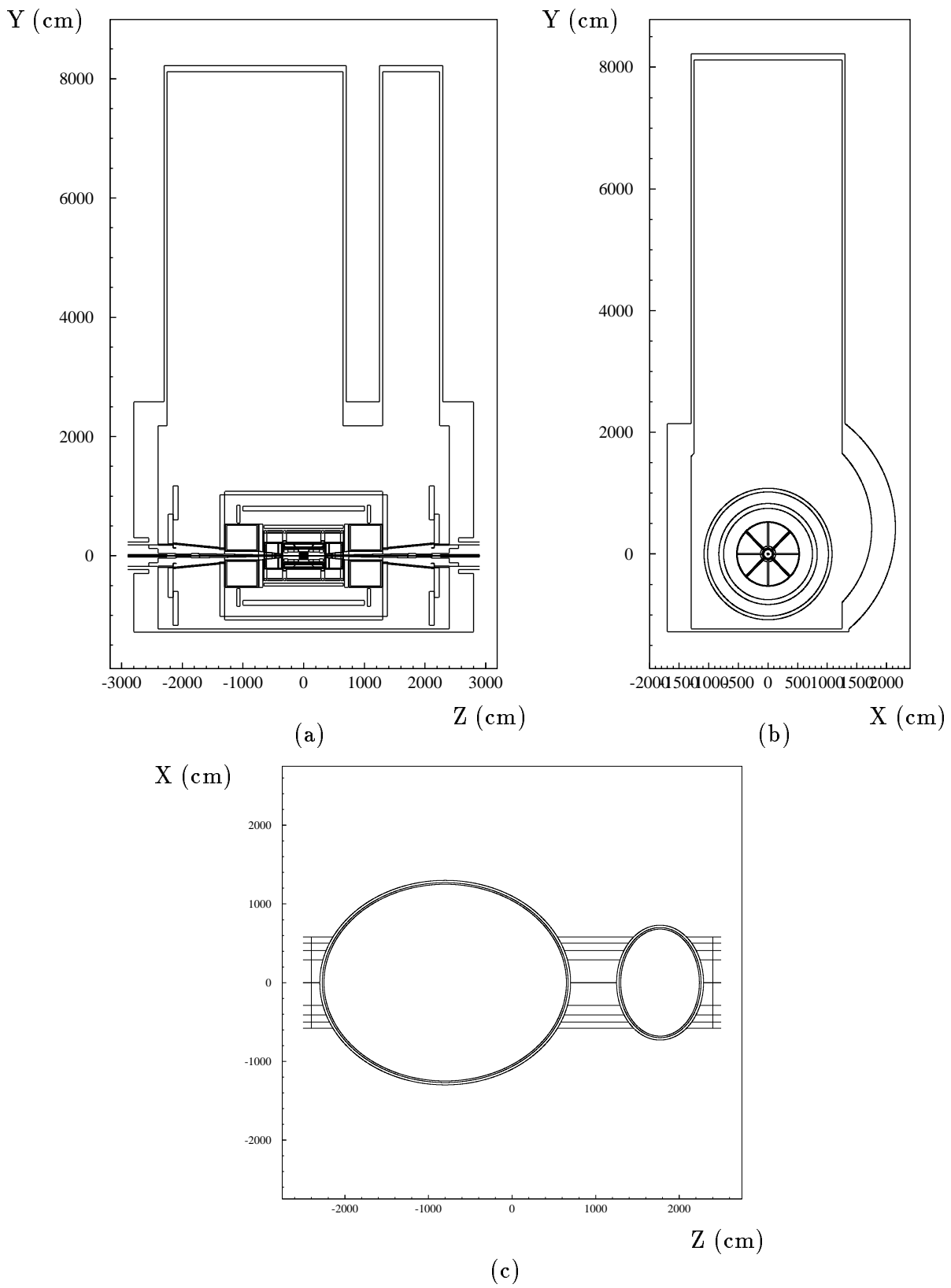


Figure 1: Sketch of the ATLAS geometry simulated in FLUKA code. Cut through the zy plane (a), through the xy plane (b) and through the zx plane (c).

## 2. Geometry description

In order to compute the lateral shielding requirements for the ATLAS experimental region, a detailed Monte Carlo simulation with the FLUKA code [2] was presented in Ref. [3]. The detector description adopted there was the same as in the Technical Proposal [1] but it was inserted in a cylindrically symmetric experimental cavern, without openings.

In this report a more realistic geometrical description of the 48 m long hall, with two elliptical vertical shafts is used.

A cross section in the  $zy$  plane at  $x=0$  is sketched in Fig. 1a, where the  $z$ -axis points to the right, the  $y$ -axis up and the  $x$ -axis into the paper. A cut through the  $xy$  plane in the center of the big shaft ( $z=-8$  m) showing the real cavern geometry with a lateral flat vertical wall, is shown in Fig. 1b. In this figure the  $x$ -axis points to the right, the  $y$ -axis up and the  $z$  axis out of the paper. A cut through the elliptical shafts ( $29 \times 25$  and  $13.6 \times 9.4$   $m^2$ ) in the  $zx$  plane, at  $y=25$  m, is shown in Fig.1c.

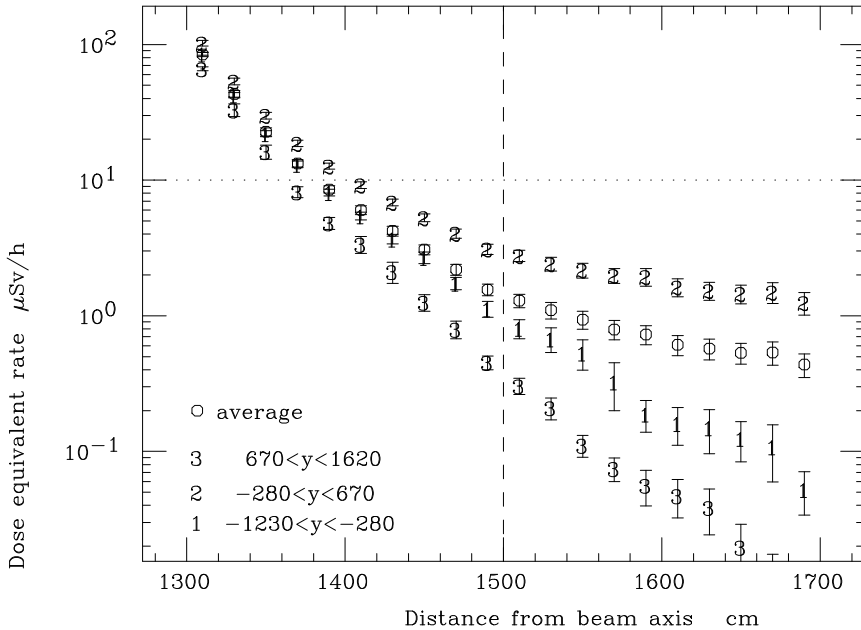


Figure 2: Dose equivalent rate, averaged over the whole wall length, versus the distance from the beam line. Together with the average over the wall height the different contributions coming from the three different vertical regions are plotted. The first surface of the concrete wall is at 1300 cm, the dashed line is at 200 cm depth.

The height between the beam axis and the natural external ground surface is 81.2 m.

The distance between the flat vertical wall and the beam is 13 m, while the curved wall

is slightly further away. In the latest version of the ATLAS cavern both walls are essentially flat but this is not expected to have any significant impact on the estimates reported here.

### 3. Lateral wall

With the geometry described above, the total dose rate in the lateral concrete wall has been computed. The analysis presented here concerns the vertical flat wall since it is the closest to the beam line. The value of the averaged surface dose at this wall is very similar to the result previously obtained using a model with a symmetrical cylindrical wall [3]. The relative contributions coming from the different kinds of particles are also very similar.

In the present analysis the vertical wall has been divided into three horizontal strips along the complete length of the hall, each strip is 9.5 m high. The lowest one, starting from the floor ( $y=1$ ), a central one at the beam level ( $y=2$ ) and an upper one up to the ceiling ( $y=3$ ). As expected, the maximum dose rate versus the distance from the beam axis, inside the concrete wall, occurs in the central region, since it is the closest to the beam, as shown in Fig. 2, while the average over the whole wall is lower than this maximum by about a factor of two.

Fig. 3 shows the dose equivalent rate inside the flat wall versus the length of the cavern for each of the three regions. The variation in the  $z$  direction is not very pronounced but the presence of weak points in the internal detector shielding is noticeable in the  $y=2$  strip. The dashed line represents the two metres of concrete needed to reduce the dose level below the  $10 \mu\text{Sv/h}$  limit allowed for a controlled area. As can be seen in Fig.3 ( $y=2$ ) the two meters of concrete are sufficient to bring the dose rate below the  $10 \mu\text{Sv/h}$  limit in the central region ( $z \pm 10$  m) where the counting room is located. The required wall thickness for CMS is larger (3 m) and the reason for this is discussed in Ref. [4].

### 4. Vertical shafts

Since the dimensions of the shafts are huge, the universal curves [5] usually used to calculate the attenuation in a maze with one or more legs may not be reliable and hence the neutron and photon flux in the two shafts was estimated with a FLUKA simulation. As shown in Fig. 7 the neutron flux changes by nine orders of magnitude between the central region of the detector and the top of the shafts. The neutron energy spectrum also changes from the bottom to the top of the shaft (Fig. 4), because of the attenuation due to air. As a result the overall uncertainty in the final results could be higher than the usual factor of two assumed for the dose estimations in the experimental cavern itself.

The calculated dose rate in the top plugs of both shafts versus the concrete thickness is shown in Fig. 5.

In order to investigate if the dose attenuation along the shafts could be approximated

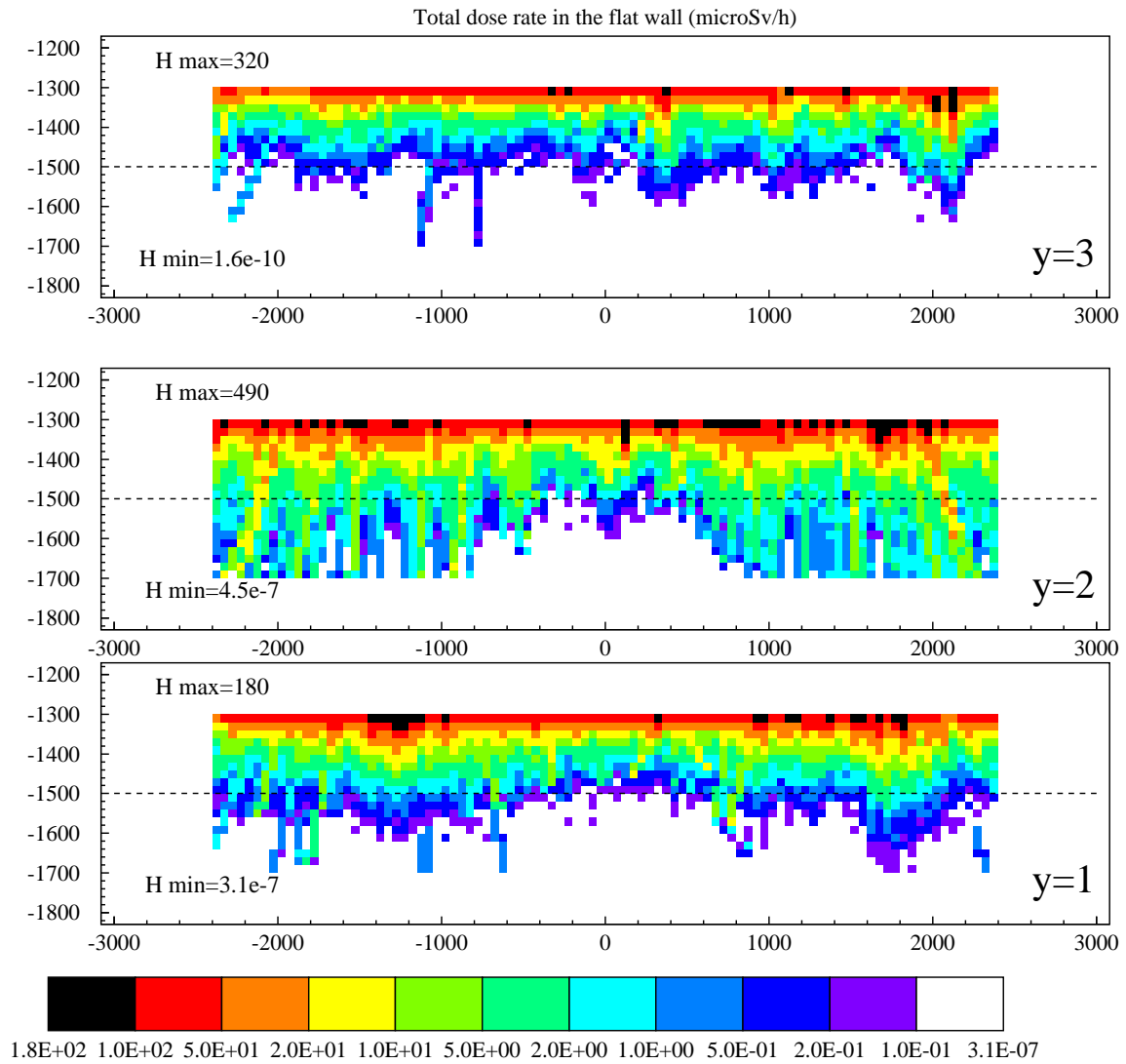


Figure 3: The dose equivalent rate ( $\mu\text{Sv/h}$ ) inside the flat wall versus the length of the cavern for each of the three 9.5 m high horizontal regions. The lowest one  $y=1$  from the floor up,  $y=2$  covers the beam height and  $y=3$  corresponds to the uppermost 9.5 m to the roof.

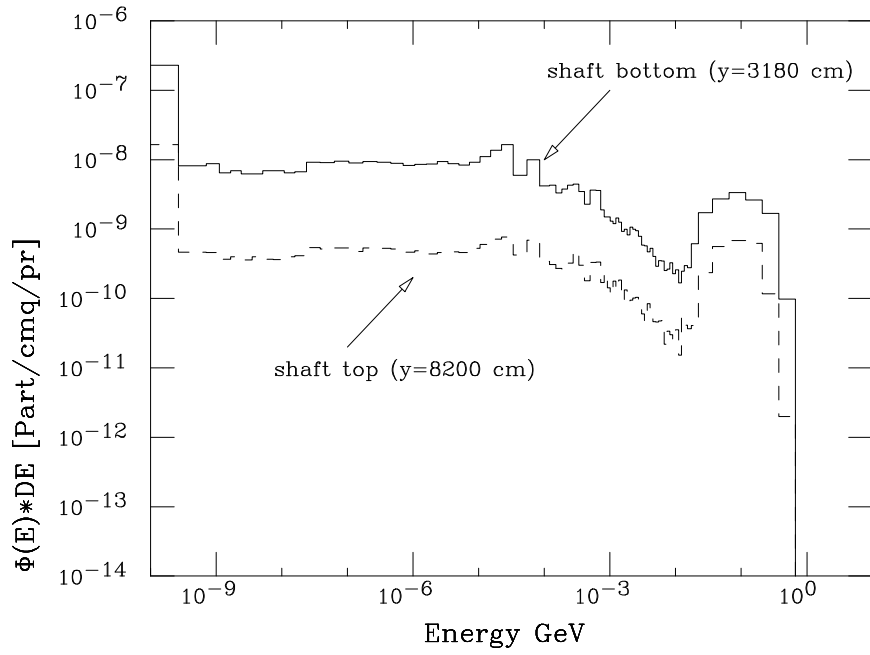


Figure 4: Neutron spectrum at the bottom and at the top of the big shaft.

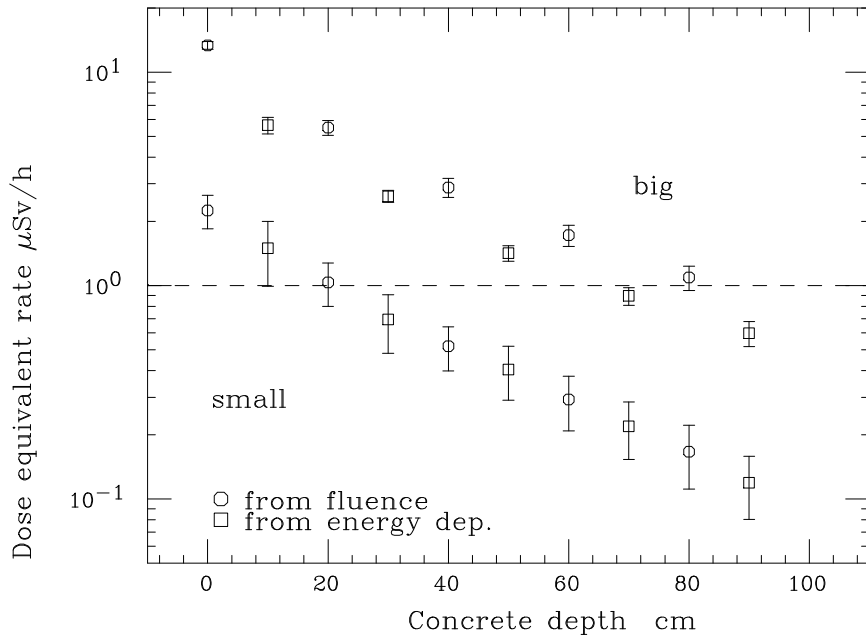


Figure 5: Total dose equivalent in the top plugs of the shafts

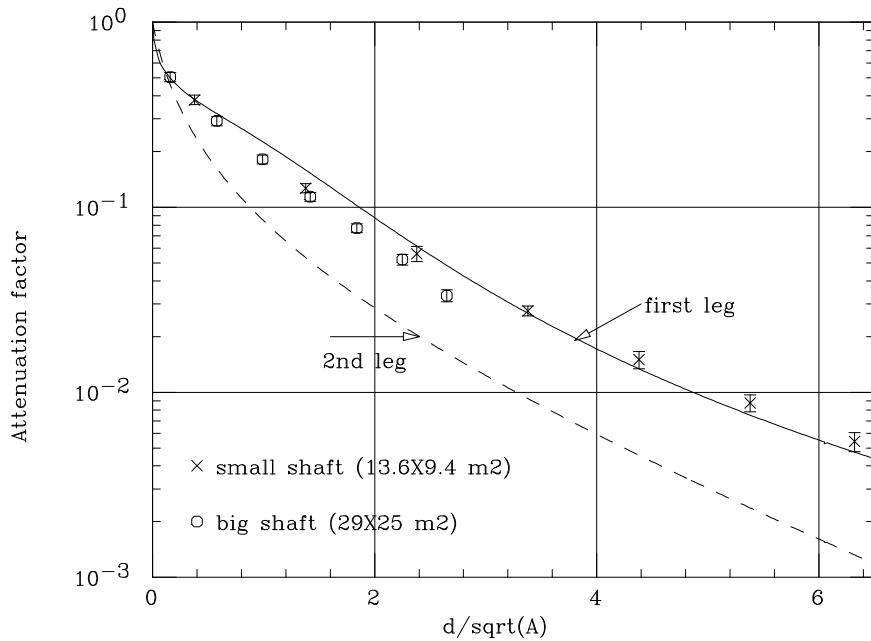


Figure 6: Calculated attenuation factor in the two shafts compared to the attenuation factor given by the universal curves.

by the universal curves for a maze with one leg, Fig. 6 shows the attenuation factor versus  $d/\sqrt{A}$ . For both shafts the universal curve is a reasonable approximation to the attenuation up the shaft, but the normalisation, or source term remains a problem, since it is unclear where the cavern stops and the shaft starts. It appears that attenuation up the larger shaft is indeed somewhat greater than predicted by the universal curve.

The neutron fluence on the external surface, without any additional top of the shaft shielding is shown in Fig. 7. The fluence with an 80 cm concrete plug for the big shaft and a 40 cm for the small one, has also been computed and the resulting dose levels are shown in Fig. 8.

From these figures it is possible to see that with such a thickness the dose where the surface buildings will be located is below the  $1 \mu\text{Sv/h}$  level allowed for a surveyed area and substantially below  $0.1 \mu\text{Sv/h}$  at the site fence (100 m apart). Taking into account a safety factor the final thickness of the plugs should be 120 cm of concrete equivalent for the big one and 80 cm for the smaller one. These thicknesses are expected to be adequate for the ultimate LHC performance which will only be achieved after many years, if at all.

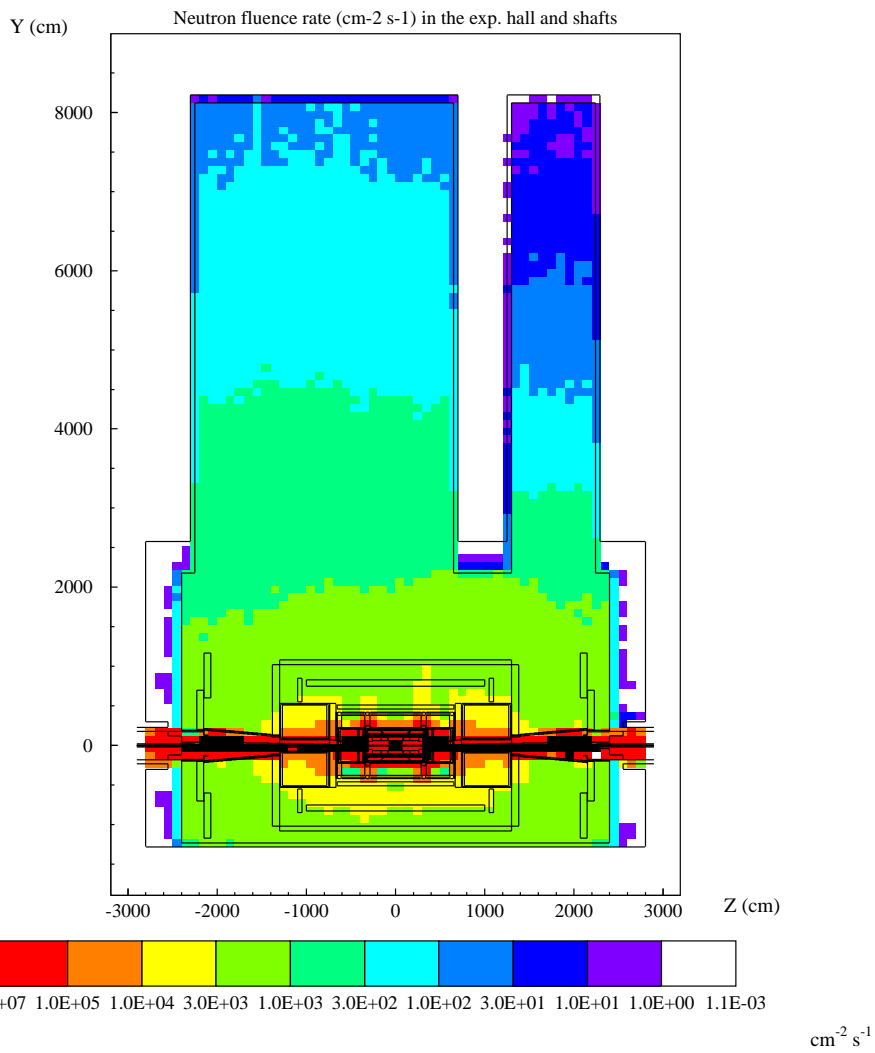
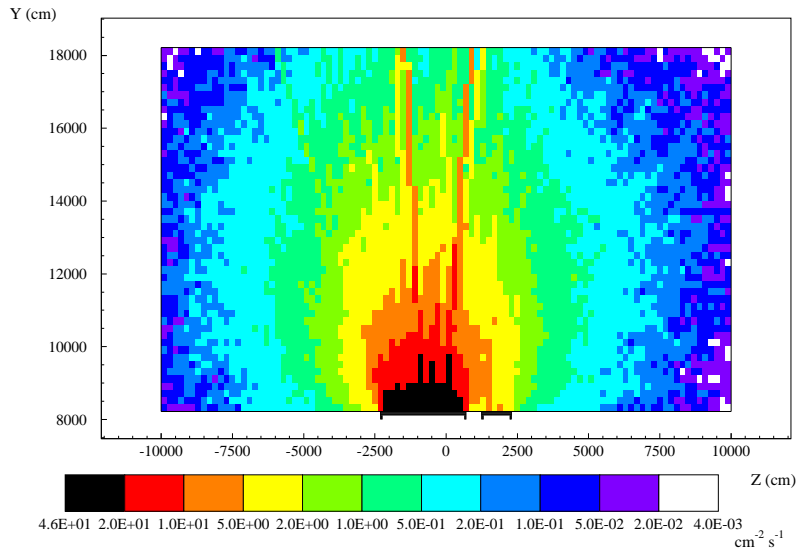


Figure 7: Neutron fluence rate ( $\text{cm}^{-2}\text{s}^{-1}$ ) in the experimental area and in the vertical shafts (lower) and on the external surface, without concrete plugs (upper). All the numbers are normalized to  $10^9$  p/s.



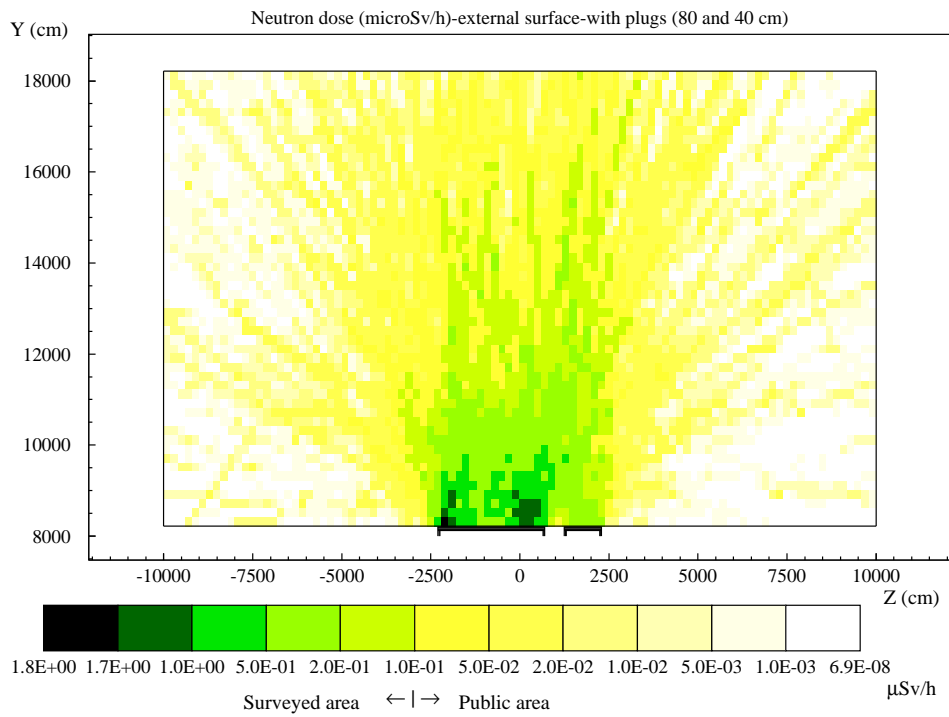
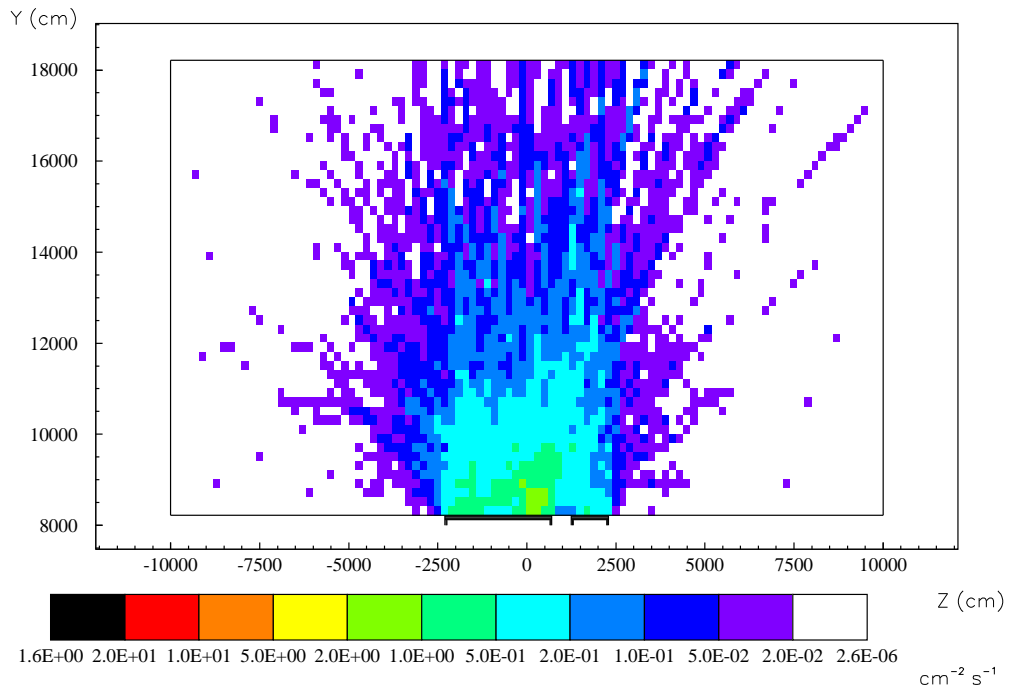


Figure 8: Neutron fluence rate ( $\text{cm}^{-2}\text{s}^{-1}$ ) on the external surface with concrete plugs (80 cm for the big shaft and 40 cm for the small one) (upper) and the corresponding dose equivalent rate ( $\mu\text{Sv/h}$ ) (lower). All the numbers are normalized to  $10^9$  p/s.

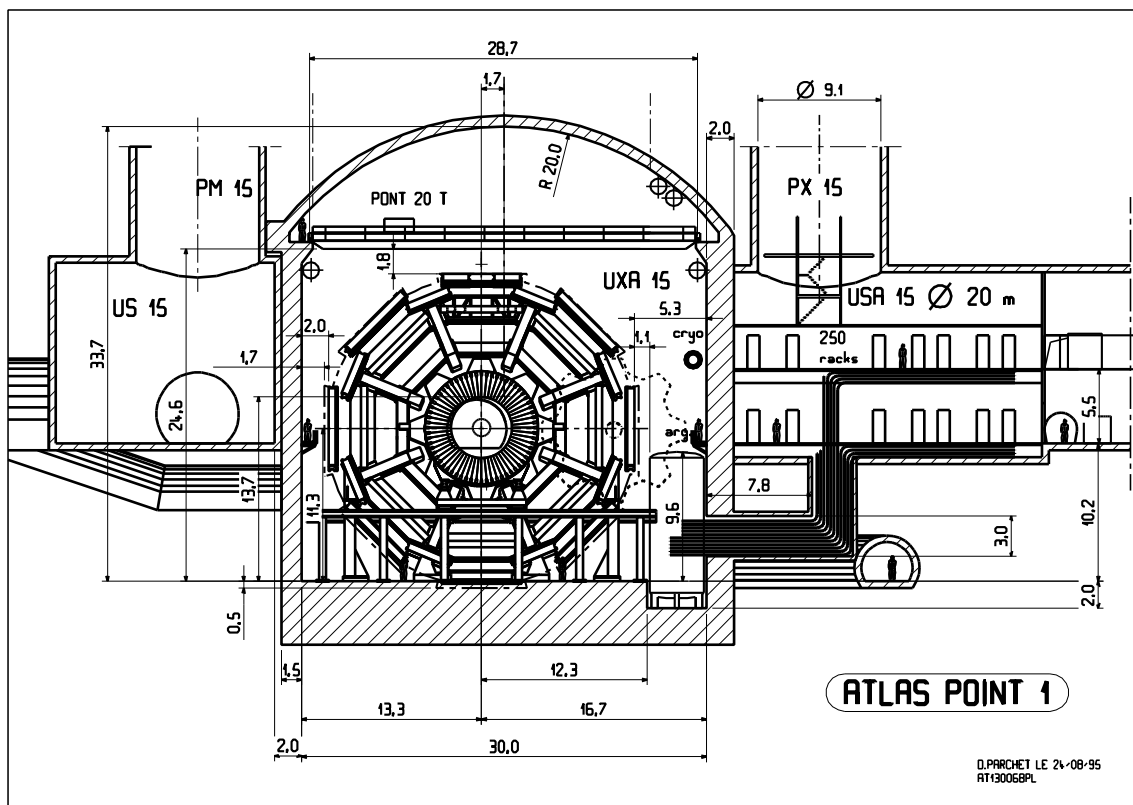
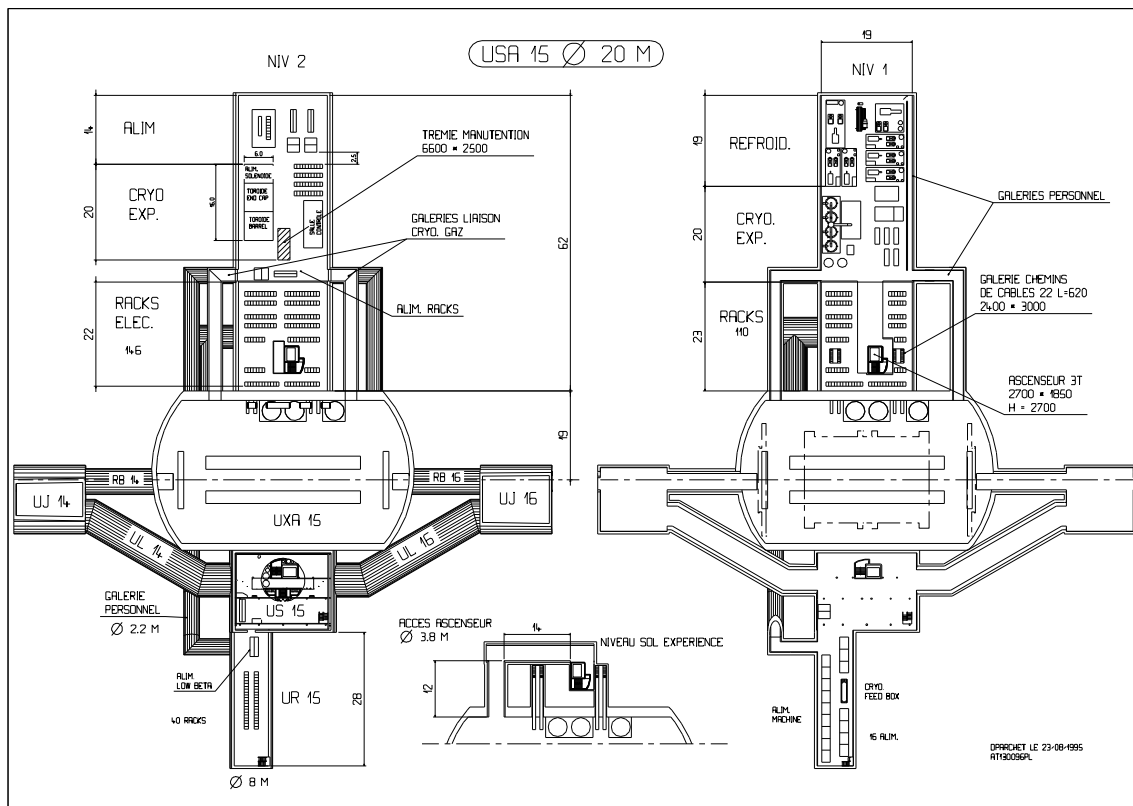


Figure 9: Passages for cables and personnel in ATLAS

	width	height	d1	d2	$\frac{d1}{\sqrt{A}}$	$\frac{d2}{\sqrt{A}}$	attenuation factor (point source off-axis)			att. factor (line source)
	(m)	(m)	(m)	(m)			1st leg	2nd leg	total	total
cables										
(option a)	2.4	3.0	7.8	4.4	2.91	1.64	$3.9 \cdot 10^{-2}$	$4.0 \cdot 10^{-2}$	$1.6 \cdot 10^{-3}$	$2.8 \cdot 10^{-3}$
(option b)	"	"	"	3.4	2.91	1.26	$3.9 \cdot 10^{-2}$	$6.1 \cdot 10^{-2}$	$2.4 \cdot 10^{-3}$	$4.3 \cdot 10^{-3}$
(option c)	"	"	"	2.4	2.91	0.89	$3.9 \cdot 10^{-2}$	$9.8 \cdot 10^{-2}$	$3.8 \cdot 10^{-3}$	$6.9 \cdot 10^{-3}$
personnel (floor level)	3.8	2.9	12.0	12.0	3.61	3.61	$2.2 \cdot 10^{-2}$	$7.8 \cdot 10^{-3}$	$1.7 \cdot 10^{-4}$	$3.1 \cdot 10^{-4}$
personnel (beam level)	2.4	2.3	25.0	8.0	10.64	3.41	$1.0 \cdot 10^{-3}$	$9.1 \cdot 10^{-3}$	$9.3 \cdot 10^{-6}$	$5.4 \cdot 10^{-5}$
cryogenics and gas pipes	2.5	2.5	25.	3.0	10.0	1.20	$1.2 \cdot 10^{-3}$	$6.6 \cdot 10^{-2}$	$8.1 \cdot 10^{-5}$	$3.3 \cdot 10^{-4}$
(upper level)	2.4	2.4	13.0	—	5.42	—	$7.4 \cdot 10^{-3}$	—	$7.4 \cdot 10^{-3}$	$1.8 \cdot 10^{-2}$
personnel (to US15)	2.4	2.3	20.5	7.5	8.73	3.19	$1.8 \cdot 10^{-3}$	$1.1 \cdot 10^{-2}$	$2.0 \cdot 10^{-5}$	$6.6 \cdot 10^{-5}$

Table 1: Dose attenuation factors given by the different kinds of passages and ducts between the experimental hall and the side caverns.

## 6. Passage ways and cable ducts

It has been decided that all the equipment to be installed underground for the cryogenics, gas distribution, electric power and cooling systems will be located in the same underground cavern as the electronics of the experiment. The present design (Ref. [6]) has a cavern (USA15) of 20 m diameter and 62 m length, with the axis perpendicular to the experimental cavern, Fig. 9. The final layout it is not completely defined and fixed but the type, number and dimensions of the passages connecting the experimental hall and the lateral cavern will not be too different from the ones sketched in Fig. 9. At the floor level of the experimental cavern a passage way for personnel and two ducts for cables are foreseen, their dimensions and lengths are presented in Table 1.

Another two passages for personnel access are at beam level, while two ducts for cryogenics and gas pipes are positioned at the level of the second floor of the lateral cavern. A single passage for personnel is also required to connect the central cavern with the other lateral cavern (US15) where the machine and power supplies will be located.

Since the agreed 2 m thick concrete wall gives an attenuation of  $1.8 \cdot 10^{-2}$ , all the passages between the experimental cavern and the lateral room must give at least the same attenuation. In fact, since ducts are necessarily of relatively small dimensions at their entry point, the attenuation factor should be adequate for the highest dose on the wall rather than the average.

The universal curves have been used to make estimates of the attenuation provided by the proposed ducts and passages as summarized in Table 1. In this table d1 and d2 are the

Diameter (m)	$A$ ( $m^2$ )	$\sqrt{A}$ (m)	$d_{min}$ (m)	attenuation (point source off axis)	attenuation (line source)
0.5	0.1963	0.4431	$\approx 5$	$8.7 \cdot 10^{-4}$	$4.0 \cdot 10^{-3}$
1.0	0.7854	0.8862	$\approx 9$	$1.2 \cdot 10^{-3}$	$4.0 \cdot 10^{-3}$
1.5	1.7671	1.3293	$\approx 14$	$1.1 \cdot 10^{-3}$	$4.0 \cdot 10^{-3}$
2.0	3.1416	1.7724	$\approx 18$	$1.2 \cdot 10^{-3}$	$4.0 \cdot 10^{-3}$

Table 2: Minimum length allowed for circular duct with different diameters.

lengths of the first and second legs respectively and  $A$  is the area of the cross section of the duct. The attenuation factors are given for a point source off the axis of the first leg and for a line source. The attenuation in the second leg is the same in both cases.

Taking into account a reasonable safety factor, the maximum dose rate at the entrance of these ducts can be taken as  $300 \mu\text{Sv/h}$ , with the above estimated attenuation factors the dose rate at the far end of most of these passages will be well below the  $10 \mu\text{Sv/h}$  allowed for a controlled area. The only one which does not provide sufficient attenuation is the single leg duct for a cryogenic line, where if a point source on its axis were to occur, unacceptably high doses might result in the equipment cavern. It is understood that this option will not be used and it is included here only to illustrate the importance of the second leg. It is extremely difficult to achieve sufficient attenuation in a single leg duct unless the cross section can be made very small. Table 2 shows the minimum lengths required to obtain adequate attenuation for different diameter ducts.

The entrance to the personnel passage at beam level is at a position where the source term is a maximum. As a result a point source on the axis of the first leg, when the attenuation is simply given by an inverse square law, has been considered. Even in this extreme case the dose at the equipment room end of the passage is below  $10 \mu\text{Sv/h}$ . Since the trigger cables must be as short as possible they can be inserted in a small single leg duct such as indicated in Table 2 or added to the other cable ducts shortening the second leg, as presented in the different options in Table 1.

## 7. Conclusions

The required thickness of the lateral wall must be equivalent to 2 m of concrete, this includes a reasonable safety factor.

The computed minimum thicknesses for the top plug of the shafts are 80 cm for the big one and 40 cm for the small. As explained care is needed with these estimates and the minimum thicknesses after applying suitable safety factors are 120 cm and 80 cm respectively.

With these two plugs the dose level in the surface building will be substantially below  $1 \mu\text{Sv/h}$  allowed for a surveyed area. The dose at the fence will be below the  $0.1 \mu\text{Sv/h}$  as required for a public area, even at the ultimate level of LHC performance.

The layout of all the passages, as currently planned, between the experimental cavern and the lateral equipment cavern gives an attenuation factor that is larger than the minimum requirement. Hence the dose in the lateral cavern will be everywhere lower than the limit of  $10 \mu\text{Sv/h}$  as required for a controlled area.

## Acknowledgments

We would like to thank A. Fassò, M. Huhtinen, G. Stevenson for discussions and help during the course of this work. Tanks are also due to G. Kantardjian and D. Parchet for their kind help and useful suggestions.

## References

- [1] ATLAS Collaboration, *Technical Proposal for a General-Purpose pp Experiment at the Large Hadron Collider at CERN*, CERN/LHCC/94-43 (1994).
- [2] A. Fassò, A. Ferrari, J. Ranft, and P.R. Sala, Proc. IV Int. Conf. on Calorimeters and their Applications, La Biodola, Isola d'Elba, September 21-26 1993, World Scientific, Singapore (1994), 493.
- [3] A. Ferrari, K. Potter and S. Rollet, *Lateral Shielding Requirements for the ATLAS Experimental Region*, CERN Internal Report CERN/AT-XA/02N/95 (1995).
- [4] M. Huhtinen and G.R. Stevenson, *Shielding Requirements in the CMS Experimental Region*, CERN Internal Report CERN/TIS-RP/IR/95-15, CERN/CMS/TN 95-056 (1995).
- [5] G. R. Stevenson, A. Fassò, *A comparison of a MORSE calculation of attenuation in a concrete-lined duct with experimental data from the CERN SPS*, Proc. Topical Conference on Theory and Practices in Radiation Protection and Shielding, Knoxville 22-24 Apr. 1987, p. 428.
- [6] ATLAS Collaboration, *Coordination pour la zone expérimentale et son infrastructure*, Compte rendu de la XIV réunion, ECP/DI/029/GK (1995).